FINITE ELEMENT ANALYSIS OF MMIC STRUCTURES USING ABSORBING BOUNDARY CONDITIONS

J. S. Wang and Raj Mittra

Electromagnetic Communication Laboratory, Department of Electrical and Computer Engineering
University of Illinois, Urbana, Illinois 61801-2991

ABSTRACT

In this paper, three-dimensional finite element method (FEM) is employed in conjunction with first and second-order absorbing boundary conditions (ABCs) to analyze waveguide discontinuities and to derive their scattering parameters. While the application of FEM for the analysis of MMIC structures is not new, to the best of the knowledge of the authors the technique for mesh truncation for microstrip lines using the first and higher-order ABCs, described in this paper, has not been reported elsewhere. Numerical solutions for two representative waveguide discontinuities are obtained and compared with published data.

INTRODUCTION

The design of monolithic microwave integrated circuits (MMIC) and electronic packages requires a knowledge of the broadband frequency response of various microstrip discontinuities. Because of the complexity of these discontinuities, it becomes necessary to use numerical modeling to compute their scattering parameters, and the finite element method (FEM) provides a very effective tool for such modeling. Two recent advances in the FEM analysis, described below, have made it even more attractive than it has been in the past. The first of these is the introduction of vector or "edge" elements, which maintain the tangential continuity of the electric and magnetic fields $\vec{E}$ and $\vec{H}$, respectively, and annihilate spurious solutions. The second is the use of local type of absorbing boundary conditions [1], which retain the sparsity of the FEM stiffness matrix. Although FEM has been employed in the past in conjunction with ABCs to solve various electromagnetic scattering problems, to-date this approach has not been utilized for full-wave analysis of microstrip and MMIC structures that require different ABCs than those employed in free-space scattering problems, because of the wave guiding nature of the microstrips. In this paper we present a full-wave analysis of complex microstrip discontinuities, based upon the edge-element FEM formulation and first and second-order absorbing boundary conditions, specially designed for microstrip structures, for mesh truncation.

FORMULATIONS USING ABCS

A typical microstrip discontinuity configuration is shown in Fig. 1. The volume Ω represents the truncated solution domain containing an arbitrarily-shaped, three-dimensional discontinuity. The open surfaces of Ω may be divided into two types, viz., the terminal planes and the side

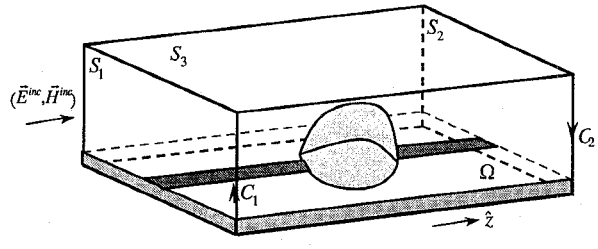

Figure 1. The truncated solution domain containing arbitrary, three-dimensional discontinuities. The surface under the dielectric substrate is the ground plane.

walls. The two terminal planes at the input and output ports, are denoted by S_1 and S_2 with boundaries C_1 and C_2, respectively. The side walls are denoted by S_3. From Maxwell's equations, we can readily show that the electric field satisfies a *curlcurl* equation, which can be transformed into the weak form:

$$\iiint_\Omega \frac{1}{\mu_r}\nabla\times\vec{E}\cdot\nabla\times\vec{W}_m dV - k_0^2\iiint_\Omega \varepsilon_r\vec{E}\cdot\vec{W}_m dV + \iint_S \frac{1}{\mu_r}\hat{n}\times\nabla\times\vec{E}\cdot\vec{W}_m dS = 0 \quad , \tag{1}$$

where $\vec{W}_m$ are the vector weighting functions, $\hat{n}$ represents the surface normal to S, $k_0 = 2\pi f\cdot\sqrt{\mu_0\varepsilon_0}$, and f is the excitation frequency. On the open surfaces, absorbing boundary conditions [1] must be applied. Because of the waveguiding nature of the guided wave structure, and the evanescent behavior of the fields along the transverse direction, different types of absorbing boundary conditions should be used on the terminal planes and the side walls.

First consider the two terminal planes, S_1 and S_2. Retaining only the dominant mode of $\vec{E}$, since the higher order modes are evanescent at the terminal planes, the transverse part of the scattered electric field can be shown to satisfy a first-order ABC

$$\left(\frac{\partial}{\partial z} \pm j\gamma\right)\vec{E}_t^s(\vec{r}) = 0, \tag{2}$$

where γ is the propagation constant of the fundamental mode, and the top and bottom signs refer to the output port (S_2) and input port (S_1), respectively. We can also define a second-

CH3277-1/93/0000-0745$01.00 © 1993 IEEE

order ABC for $\vec{E}_t^s(\vec{r})$ which reads

$$\left(\frac{\partial}{\partial z} \pm j\gamma\right)^2 \vec{E}_t^s(\vec{r}) = 0, \tag{3}$$

for a single mode, or

$$\left(\frac{\partial}{\partial z} \pm j\gamma_1\right)\left(\frac{\partial}{\partial z} \pm j\gamma_2\right)\vec{E}_t^s(\vec{r}) = 0, \tag{4}$$

for two modes where γ_1 and γ_2 are the wave numbers for these modes. Alternatively, if the ABC is required to be valid for a band of frequencies [2,3], then, for a single propagating mode at the output port, we can use

$$\left(\frac{\partial}{\partial z} + j\gamma_1^{(1)}\right)\left(\frac{\partial}{\partial z} + j\gamma_1^{(2)}\right)\vec{E}_t^s(\vec{r}) = 0, \tag{5}$$

where $\gamma_1^{(1)}$ and $\gamma_1^{(2)}$ are the propagating constants of the mode at frequencies f_1 and f_2, within the desired band.

The second-order z-derivative in the equations (3) through (5) can be replaced by a transverse operator :

$$-\frac{\partial^2 \vec{E}_t}{\partial z^2} = \nabla_t^2 \vec{E}_t + \nabla_t\left(\frac{1}{\varepsilon_r}\nabla_t \cdot \varepsilon_r \vec{E}_t - \nabla_t \cdot \vec{E}_t\right) + k_0^2 \varepsilon_r(\vec{r})\vec{E}_t, \tag{6}$$

where ∇_t^2 is the transverse part of ∇^2. When (6) is substituted into (1), the resulting expressions contain only transverse derivatives. Upon integrating by parts, the second-order transverse derivatives of $\vec{E}_t$ and the first order transverse derivatives of E_z can be eliminated and the final equation to be solved by FEM can be written as

$$\begin{aligned}
&\iiint_\Omega \frac{1}{\mu_r}\nabla \times \vec{E} \cdot \nabla \times \vec{W}_m dV - k_0^2 \iiint_\Omega \varepsilon_r(\vec{r})\vec{E} \cdot \vec{W}_m dV \\
&+\iint_{S_1+S_2} \frac{1}{\mu_r}\left[j\gamma \vec{E}_t \cdot \vec{W}_t\right]dS + \iint_{S_1} \frac{1}{\mu_r}\left[E_z\left(\nabla_t \cdot \vec{W}_t\right)\right] \\
&-\int_{C_1} \frac{1}{\mu_r}\left[E_z\left(\hat{n}_t \cdot \vec{W}_t\right)\right]dC - \iint_{S_2} \frac{1}{\mu_r}\left[E_z\left(\nabla_t \cdot \vec{W}_t\right)\right]dS \\
&+\int_{C_2} \frac{1}{\mu_r}\left[E_z\left(\hat{n}_t \cdot \vec{W}_t\right)\right]dC \\
&= \iint_{S_1} \frac{1}{\mu_r}\left[j\gamma \vec{E}_t^{inc} - \frac{\partial \vec{E}_t^{inc}}{\partial z}\right] \cdot \vec{W}_t dS
\end{aligned} \tag{7}$$

when the first-order ABC is used. Though not included here, a similar equation can be derived for the second-order ABC as well.

In addition to ABCs for the terminal planes, ABCs are also needed on the side walls of the microstrip structure and they are different from the ones given above. The tangential component of $\nabla \times \vec{E}$ on the side walls can be expressed as

$$\hat{n}_\tau \times \nabla \times \vec{E} = -\frac{\partial \vec{E}_\tau}{\partial n} + \nabla_\tau E_n. \tag{8}$$

The normal derivative in (8) can be replaced by an evanescent, first-order absorbing boundary condition

$$\left(\frac{\partial}{\partial n} + \alpha\right)\vec{E}_\tau^s(\vec{r}) = 0. \tag{9}$$

A second-order ABC, for the side walls that takes into account radiation from the discontinuities, takes the form

$$\left(\frac{\partial}{\partial n} + \alpha\right)\left(\frac{\partial}{\partial n} + jk\right)\vec{E}_\tau^s(\vec{r}) = 0. \tag{10}$$

The weak form is slightly modified when one of these side-wall ABCs, given in (9) or (10), are incorporated in (7).

NUMERICAL RESULTS

In this section, we provide illustrative numerical results for two examples. The first of these is a dielectric post discontinuity in a conventional rectangular waveguide, as shown in Fig. 2. The dielectric post has a height equal to that of the guide, b=0.5a, a width t_1=0.524a, and a length d=0.262a, where a is the width of the guide. The dielectric constant of the post is 8.2-j0.006, and l and r are the positions where the ABCs are applied. The waveguide is excited with a TE_{10} mode, whose field distribution and the propagation constant are known. We consider a frequency range from 8 to 12 GHz. We introduce the ABCs at locations that are half the waveguide width away, we choose, i.e., l=r=0.5a. The number of edges in the corresponding finite element mesh is 7138 including 2226 PEC edges. The magnitude of S_{11} vs. frequency is plotted in Fig. 3 for post length d=6, 12, 18mm, and in Fig. 4 for post length d=9, 15, 21mm. The results for d=6mm compare well with those reported in [4]. Because the propagation constant in the empty guide is known precisely, a first order ABC is found to be sufficiently accurate.

The second example considered is the junction of two microstrips by an air or dielectric bridge, shown in Fig. 5. The structure is assumed to be shielded and lossless. The microstrip has dimensions a by 0.2a, where a is a scaling factor. The substrate is GaAs with ε_{r1}=12.9. The bridge has a longitudinal dimension d, with a dielectric constant of ε_{r2}. Four different values of bridge dielectric constant, ε_{r2}=1 (air), 2.32 (organic dielectric), 3.78 (quartz glass) and 9.8 (ceramic), and three different bridge lengths, d=3.17a, 6.35a and 12.7a were considered. The purpose was to study the scattering parameters using different bridge materials and bridge lengths. The scaled frequency range under consideration ranged from k_0a=0.05 to k_0a=3.5. If a=100μm, the actual frequency range was from 24 to 166 GHz. A first order ABC was used at a position l=r=10a.

Unlike the waveguide problem discussed earlier, neither the propagation constant nor the incident field distribution of the uniform microstrip line are known in closed forms, and numerical procedures are needed to determine them. To find the propagation constant β of the input and output guides, which are identical in the present example, the uniform microstrip line can be short-circuited at both ends, and the resulting cavity problem solved to determine the propagation constant β and the model field distribution of the uniform line for a given frequency. However, this procedure

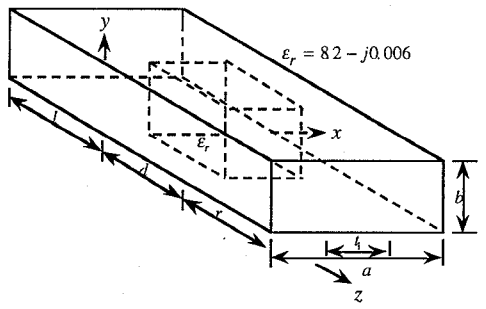

Figure 2. A centered dielectric post discontinuity in a rectangular waveguide.

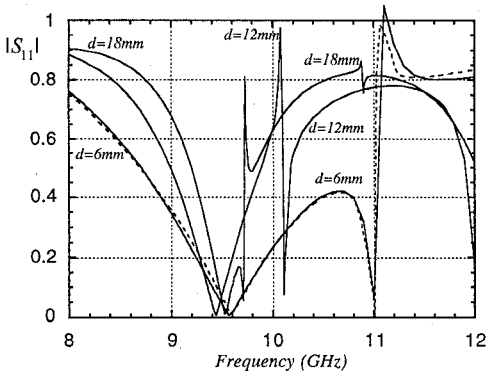

Figure 3. The magnitude of S_{11} vs. frequency for the dielectric post discontinuity problem with the length d=6mm, 12mm and 18mm. The dashed line is calculated by Uher et al [3].

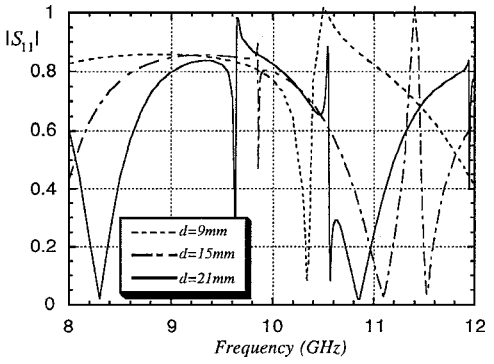

Figure 4. The magnitude of S_{11} vs. frequency for the dielectric post discontinuity problem with the length d=9mm, 15mm and 21mm.

is too costly, and we have developed a numerically-efficient procedure, described in [6], to accomplish the same objective.

Figures 6, 7 and 8 show the magnitudes of S_{11} vs. wave number k_0a with the values of the bridge dielectric constant ε_{r2} as parameters, for bridge lengths d=3.17a, 6.35a and 12.7a, respectively. The problem was solved for a total of 31 frequencies to generate each of the curves in the figures. These results were found to compare well with those obtained using the frequency domain finite difference method [5]. We

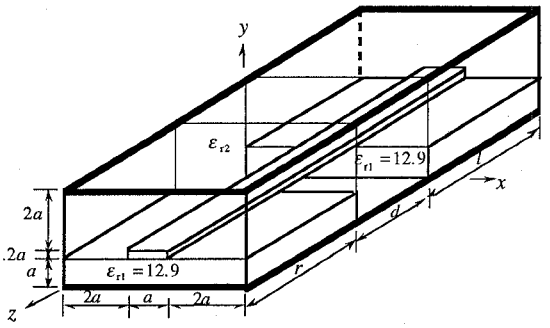

Figure 5. Junction between two microstrip lines formed by using an air or dielectric bridge.

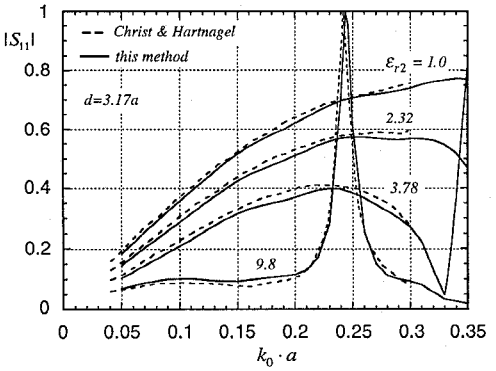

Figure 6. The magnitude of S_{11} vs. wave number k_0a with the values of the bridge dielectric constant ε_{r2} as parameters for bridge length d=3.17a.

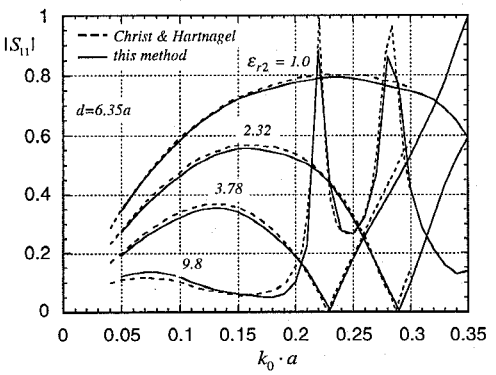

Figure 7. The magnitude of S_{11} vs. wave number k_0a with the values of the bridge dielectric constant ε_{r2} as parameters for bridge length d=6.35a.

note that one obtains improved matching for the junction for k_0a=0.05 to k_0a=0.2 when a ceramic bridge is used. However, the introduction of a dielectric bridge causes two resonances to occur, one of which has a band-stop property while the other is of the band-pass type. Increasing the bridge dielectric constant or length causes these resonant frequencies to shift toward lower frequencies.

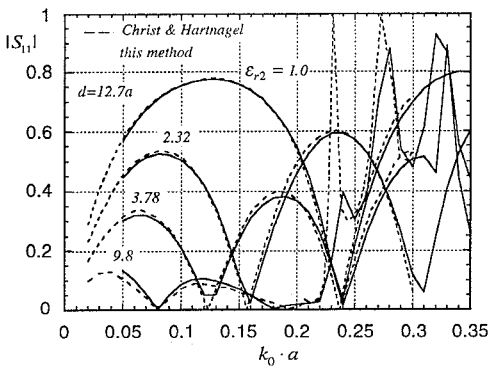

Figure 8. The magnitude of S_{11} vs. wave number k_0a with the values of the bridge dielectric constant ε_{r2} as parameters for bridge length d=12.7a.

CONCLUSIONS

In this paper we have discussed the problem of incorporating first and second-order absorbing boundary conditions in the finite element formulation to solve discontinuity problems in guided wave structures. Numerical results have been presented and have been shown to compare favorably with the published data.

ACKNOWLEDGMENT

The work reported in this paper was supported in part by the Joint Services Electronics Program under Grant N00014-90-J-1270. Support from the National Center for Supercomputing Applications at the University of Illinois for computer time on the Cray/YMP supercomputer is also acknowledged.

REFERENCES

[1] R. Mittra and O. Ramahi, "Absorbing Boundary Conditions for the Direct Solution of Partial Differential Equations Arising in Electromagnetic Scattering Problems", in Finite Element and Finite Difference Methods for Electromagnetic Scattering, M. A. Morgan Ed., New York: Elsevier, 1990, pp. 133-173.

[2] Z. Bi, Keli Wu and J. Litva, "A Dispersive Boundary Conditions for Microstrip Component Analysis Using the FD-TD Method", IEEE Trans. Microwave Theory Tech., Vol. 40, No. 4, pp. 774-777, April 1992.

[3] V. Betz and R. Mittra, "Comparison and Evaluation of Boundary Conditions for the Absorption of Guided Waves in an FDTD Simulation," submitted to IEEE Microwave and Guided Wave Letters, Vol. 2, No. 12, pp. 499-501, December, 1992.

[4] J. Uher, F. Arndt and J. Bornemann, "Field Theory Design of Ferrite-Loaded Waveguide Nonreciprocal Phase Shifters with Multisection Ferrite or Dielectric Slab Impedance Transformers", IEEE Trans. Microwave Theory and Tech., Vol. MTT-35, No. 6, pp. 552-560, June 1987.

[5] A. Christ and H. L. Hartnagel, "Three-Dimensional Finite Difference Method for the Analysis of Microwave-Device Embedding", IEEE Trans. Microwave Theory and Tech., Vol. MTT-35, No. 8, pp. 688-696, August 1987.

[6] J. S. Wang and R. Mittra, "Finite Element Analysis of MMIC Structures and Electronic Packages Using Absorbing Boundary Conditions," submitted to MTT.